The Human T-Cell Lymphotropic Virus Type-I Dimerization Initiation Site Forms a Hairpin Loop, Unlike Previously Characterized Retroviral Dimerization Motifs†

Tom P. Monie,‡,|| Jane S. Greatorex,‡ Martin Zacharias,§ and Andrew M. L. Lever*,‡

Department of Medicine, University of Cambridge, Level 5, Addenbrooke's Hospital, Cambridge CB2 2QQ, U.K., and School of Engineering and Science, International University Bremen, Campus Ring 1, D-28759 Bremen, Germany

Received November 13, 2003; Revised Manuscript Received February 18, 2004

ABSTRACT: The formation of genomic RNA dimers during the retroviral life cycle is essential for optimal viral replication and infectivity. The sequences and RNA structures responsible for this interaction are located in the untranslated 5′ leader RNA, along with other cis-acting signals. Dimer formation occurs by specific interaction between identical structural motifs. It is believed that an initial kissing hairpin forms following self-recognition by autocomplementary RNA loops, leading to formation of an extended stable duplex. The dimerization initiation site (DIS) of the deltaretrovirus human T-cell lymphotropic virus type-I (HTLV-I) has been previously localized to a 14-nucleotide sequence predicted to contain an RNA stem loop. Biochemical probing of the monomeric RNA structure using RNAse T1, RNAse V1, RNAse U2, lead acetate, and dimethyl sulfate has led to the generation of the first structural map of the HTLV-I DIS. A comprehensive data set of individual nucleotide modifications reveals that the structural motif responsible for HTLV-I RNA dimerization forms a trinucleotide RNA loop, unlike any previously characterized retroviral dimerization motif. Molecular modeling demonstrates that this can be formed by an unusual C:synG base pair closing the loop. Comparative phylogeny indicates that such a motif may also exist in other deltaretroviruses.

Retroviruses are unique among viruses in possessing a fully diploid genome consisting of two identical genomic RNA strands joined noncovalently near their 5′ termini at a location termed the dimer linkage site (DLS) (*1*, *2*). Dimer formation is conserved throughout the retroviridae, implying that it has a critical role in viral replication. In some cases, it appears that linkage between the two strands is a two-stage process with an initial interaction between canonical base pairs leading to an extended duplex formation. It has also been observed that early dimers have a relatively low affinity, whereas those found in mature virus particles have a considerably higher affinity. It is not clear whether this is directly linked to the two-stage annealing process or whether the high-affinity dimer is the result of interaction with additional factors such as viral proteins and/or additional links between the two genomic strands. Dimerization has been shown to influence viral RNA packaging (*3*−*6*), reverse transcription (*5*, *7*), and translational control (*8*). Mutations within the human immunodeficiency virus type 1 (HIV-1) region at which dimerization is initiated (the dimer initiation site, DIS) have been shown to impair viral replication (*5*, *9*), although nearby mutations can restore wild-type levels of replication (*10*, *11*).

The sequences and structures responsible for initiating dimer formation are located almost exclusively at the 5′ end of the genome in the leader RNA, within a complex array of RNA structural motifs with regulatory functions. Exceptionally, regions at the 3′ end of the genome have been implicated. The autocomplementary sequences responsible for the initial canonical pairing form through what is termed a "kissing loop" interaction (*12*−*16*).

The DIS of HTLV-I has been localized to an RNA motif between nucleotide positions 730−743, numbering from the cap site (*17*−*19*). Computer modeling predicts this motif to form a 5-base-pair helix closed by a trinucleotide loop (Figure 1). Trinucleotide loops are relatively uncommon, and they have not been previously associated with retroviral dimerization. They have been identified in RNA structures such as the domain IIId terminal loop of the hepatitis C virus internal ribosome entry site (IRES) (*20*), and in stem loops required for initiation of transcription within the Bromoviridae (*21*).

In the HCV IRES, a GU trans-wobble pair, an S-turn motif similar to that seen in the HIV-1 RRE (*22*), creates a helical structure closed by a UGG loop, forming a U-turn. In the Bromoviridae, trinucleotide loops result either from the formation of transloop base-pairing interactions in a hexanucleotide loop (*23*) or from stacking interactions at the terminus of a stable hairpin (*21*). The unusual nature of the trinucleotide loop predicted for the HTLV-I DIS compared to dimerization motifs modeled for other retroviruses (*24*, *25*) led us to undertake chemical and enzymatic probing of

† The authors acknowledge the scientific input of the HTLV European Research Network (HERN; Grant No. BMH4-CT98-3781) and the Sykes Trust. This work was funded by the Medical Research Council.

* Corresponding author. Tel.: +44-1223-330191. Fax: +44-1223-763401. E-mail: amll1@mole.bio.cam.ac.uk.

‡ University of Cambridge.

§ International University Bremen.

|| Current address: Biophysics Section, Department of Biological Sciences, Imperial College London, South Kensington Campus, London SW7 2AZ, UK.

10.1021/bi030237i CCC: $27.50
Published on Web 04/27/2004

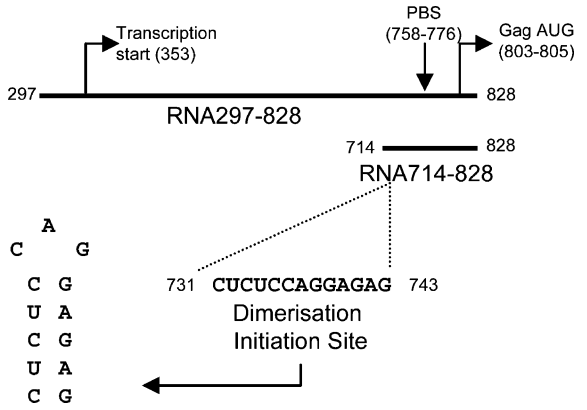

FIGURE 1: Details of RNA constructs. RNA transcripts used during the structural probing studies. Numbering of the viral sequence follows that of Ratner et al., 1991 (*32*). The transcription start site, the primer binding site (PBS), the Gag start codon, and the dimerization initiation site are identified. A computer-predicted structure for the dimerization initiation site is included.

the structure of this region to produce a map of the HTLV-I DIS. The modification patterns support the computer prediction and, in conjunction with the molecular modeling, suggest that an unusual terminal structure involving a C:synG base pair may be present to form a loop-closing pair.

EXPERIMENTAL PROCEDURES

RNA Production. The RNA constructs used during this study are identified in Figure 1. RNA297-828 has been described previously and was called RNA531 (*17, 19*). RNA714-828 was produced by SP6-mediated transcription of *Nhe*I-linearized pGEM11Δ713 (*19*). Freshly transcribed RNA was purified by ethanol precipitation and size exclusion chromatography through G-50 Sephadex columns. [γ-^{32}P]ATP end-labeled RNA714-828 was produced by a standard dephosphorylation and rekinasing reaction, incorporating 20 μCi of [γ-^{32}P]ATP (3000 Ci/mmol, 10 mCi/ml; Amersham Pharmacia Biotech).

RNA Structure Probing. Target RNA, resuspended in water, was denatured for 3 min at 80 °C and snap-cooled on ice before probing to ensure a single conformational population of monomeric RNA. Primer extensions were performed with 1.0 μg of RNA714-828 or RNA297-828 per sample, and end-labeled probing with 1 μg of RNA714-828 per sample.

(a) RNAse T1. RNA was diluted, on ice, in 2× T1 probing buffer (100 mM cacodylic acid [pH 7.0], 200 ng/μL yeast tRNA, 4 mM $MgCl_2$). A 1.0-μL volume of RNAse T1 (Ambion), diluted in 100 mM cacodylic acid, at a concentration of 2.5 or 5.0 U/μL, was added in a total reaction volume of 50 μL. Samples were incubated on ice for 30 min and then terminated, and the RNA was precipitated by addition of 150 μL of 100% EtOH.

(b) Dimethyl Sulfate (DMS). RNA was diluted with 2× DMS probing buffer (140 mM Hepes−KOH [pH 7.8], 20 mM $MgCl_2$, 540 mM KCl, 2 mM DTT) to a volume of 200 μL, 20 μL of 10% DMS (Fluka) (diluted in 50% EtOH) was added, and samples were incubated for 10 min at 30 °C. Reactions were terminated, and the RNA was precipitated with 10 μg of yeast tRNA, 50 μL of DMS stop mix (1 M Tris-HCl [pH 7.5], 1 M β-mercaptoethanol, 0.1 mM EDTA), and 675 μL of 100% EtOH.

(c) Lead Acetate. Master mixes were prepared with a composition per 8.0 μL of 1.0 μg of target RNA, 5.0 μg of yeast tRNA, and 2.0 μL of lead probing buffer (100 mM Hepes−NaOH [pH 7.5], 25 mM magnesium acetate, 250 mM potassium acetate). This was incubated for 5 min at room temperature and dispensed into 8.0-μL aliquots, and 2.0 μL of freshly prepared lead acetate (1, 2, or 4 mM, diluted from 100 mM stock) (Sigma) was added. Samples were incubated for a further 5 min at room temperature and then quenched and precipitated with 5.0 μL of 0.1 M EDTA, 1.5 μL of 3 M sodium acetate [pH 5.3], and 50 μL of 100% EtOH.

Precipitated RNA was resuspended in either 2 or 4 μL of H_2O, and 1 μL was used as a template for reverse transcription. Modified or cleaved RNA was annealed with 50 pmol of the DNA oligonucleotide primer 802-783 (50 pmol/μL; GCCTAGGGAATAAAGGGC; Sigma-Genosys) in TK buffer (30 mM Tris-HCl [pH 7.5], 50 mM KCl) by incubation at 70 °C for 5 min and slow cooling to 42 °C. Control reactions were set up, for reverse transcription and the determination of natural pause sites, using 1.0 μg of unmodified monomeric RNA. A 2-μL volume of each RNA:primer annealed complex was removed, and to this was added 3 μL of extension mixture (12.5 mM Tris-HCl [pH 8.3], 50 mM KCl, 25 mM $MgCl_2$, 10 mM DTT, 5 μM dTTP, 0.5 mM dATP, 0.5 mM dCTP, 0.5 mM dGTP, 2.0 μCi of [α-^{32}P]dTTP (3000 Ci/mmol, 10 mCi/mL; Amersham Pharmacia Biotech), 8 units of RNAsin (Promega), 40 units of Moloney Murine Leukaemia Virus Reverse Transcriptase (Promega)). Reverse transcription was allowed to proceed for 15 min at 42 °C and then chased with 1.0 μL of 1.8 mM dTTP for a further 15 min before quenching with 3 μL of Gel Loading Buffer II (Ambion). cDNA was denatured for 5 min at 95 °C, prior to resolution by 10% or 12% polyacrylamide gel electrophoresis. Cycle sequencing ladders were generated from the appropriate DNA template using the oligonucleotide primer 802-783 and the femtomole DNA Cycle Sequencing System (Promega) per the manufacturer's instructions.

(d) RNAse V1. A 0.2-μg amount of [γ-^{32}P]ATP 5′ end-labeled RNA714-828 was probed with RNAse CV_1 (Amersham Pharmacia). The reaction was performed in 2× CV_1 buffer (20 mM Tris [pH 8], 4 mM $MgCl_2$, 0.2 M KCI). Enzyme was diluted to 0.1, 0.05, and 0 U/μL on ice in 2× CV_1 buffer. A 1-μL volume of diluted enzyme was added to the RNA in a 50-μL reaction also containing 10 μL of yeast tRNA. Reactions were incubated for 20 min on ice and stopped by addition of ethanol. Precipitated RNA was redissolved in water after washing in 95% ethanol loading buffer, and electrophoresis was performed as described above. An alkaline hydrolysis ladder of the RNA transcript was made to act as a marker.

(e) RNAse U2. RNA was as for the RNAse CV_1 experiments. The enzyme (Amersham Pharmacia) was dissolved in water to 10 U/μL. For reactions, it was diluted in water on ice to 0.1, 0.2, and 0 U/μL. Reactions were carried out in 20-μL volumes containing RNA, 20 mM sodium acetate (pH 4.8), 2 mM $MgCl_2$, 100 mM KCI, 10 μg of yeast tRNA, and enzyme dilution. After 20 min on ice, 30 μL of water was added, and RNA precipitation, etc., was carried out as for RNAse T1 above.

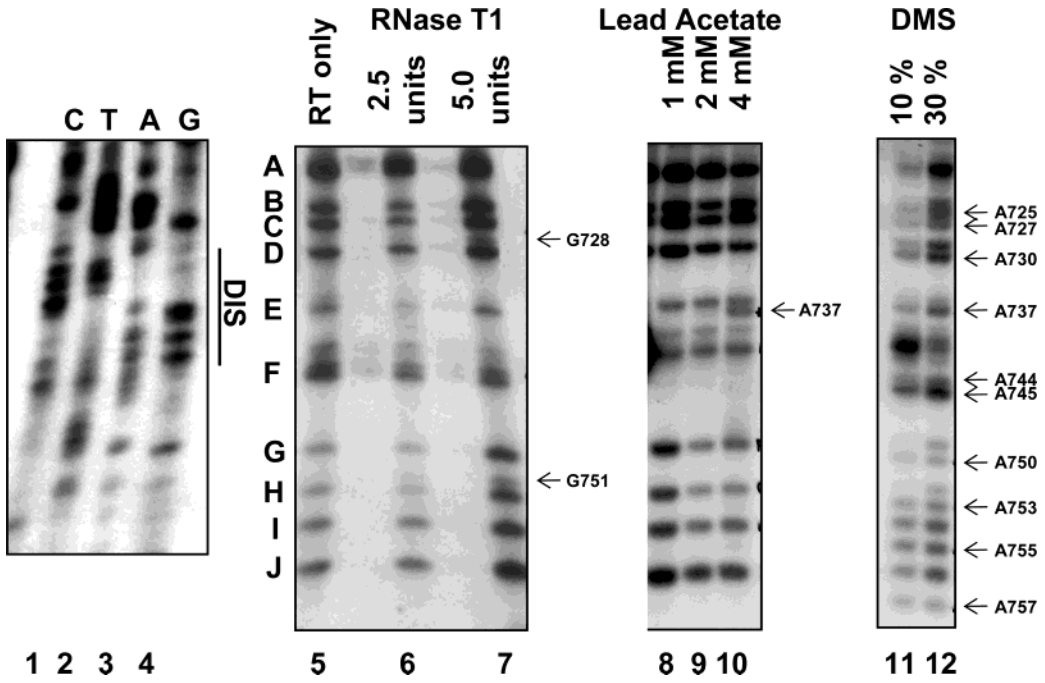

FIGURE 2: Probing the RNA secondary structure of the HTLV-I DIS by primer extension. Lanes 1−4, cycle sequencing ladder of the HTLV-I DIS region; lane 5, control for natural reverse transcriptase pausing on unmodified monomeric RNA. Monomeric HTLV-I leader RNA was enzymatically and chemically probed with 2.5 units of RNAse T1 (lane 6), 5.0 units of RNAse T1 (lane 7), lead acetate at final concentrations of 1 (lane 8), 2 (lane 9), and 4 mM (lane 10), and also 10% DMS (lane 11) and 30% DMS (lane 12). Positions of base modification are marked by an arrow and numbered to the right of each panel, while natural reverse pausing events are identified on the left-hand side.

RESULTS

Structural Mapping of the HTLV-I DIS. The core HTLV-I DIS (positions 730−743) can mediate dimer formation between short RNA sequences (*19*). To determine the structures of RNA elements involved in the proposed atypical DIS, we performed chemical and enzymatic probing on the viral transcripts RNA714-828 and RNA297-828. RNA was denatured prior to modification to ensure homogeneous monomeric conformation. Representative gels of modification patterns are provided in Figures 2 and 3, and a structural map is presented in Figure 4.

Natural RT pausing on an RNA template is promoted by secondary structural elements and homopolymeric adenine sequences (*26*). In vitro, these pause sites are highly reproducible and provide important information on the native RNA structure, complementing that from direct modification. They also provide reproducible sites for orientation of the sequence comparable to a sequence ladder. Reverse transcription, initiated from the DNA oligonucleotide 802-783, produced a series of highly reproducible pauses across the DIS region (Figure 2, lane 5). The individual nucleotides associated with these pauses were identified by alignment against cycle sequencing ladders (Figure 2, lanes 1−4). Pauses could be predominantly attributed to specific adenine residues, with the resultant pattern being consistent with the presence of a structural motif in the region of the DIS.

The HTLV-I DIS contains four guanine residues, three of which (G739, G741, and G743) have a predicted involvement in Watson−Crick base pairing, and the fourth (G738) forms part of a trinucleotide terminal loop (Figure 1). Enzymatic probing with RNase T1, specific for unpaired guanines, produced no cleavage within the DIS (Figure 2, lane 6) but did cleave both G728 and G751 (Figure 2, lane 7). This modification pattern supports the postulated helical stem but strongly suggests that G738 is not in single-stranded conformation.

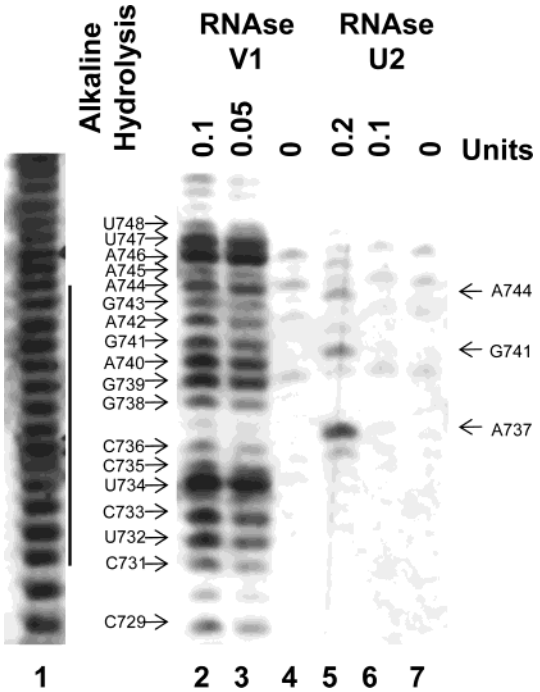

FIGURE 3: Modification of end-labeled HTLV-I RNA. A 0.05-μg amount of monomeric end-labeled RNA714-828 was modified with either RNAse V1 (lane 2, 0.1 U; lane 3, 0.05 U; lane 4, 0 U) or RNAse U2 (lane 5, 0.2 U; lane 6, 0.1 U; lane 7, 0 U). An alkaline hydrolysis ladder of the RNA was run in parallel to isolate specific bases (lane 1). The DIS motif is delineated by a vertical solid bar, and the corresponding nucleotides are identified.

Modification of monomeric RNA714-828 and RNA297-828 with lead acetate induced strong, specific cleavage of

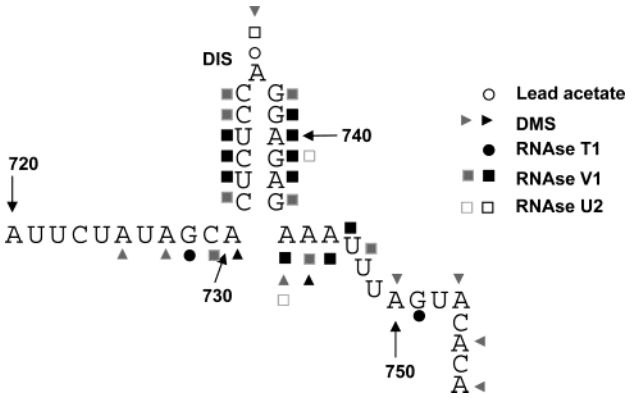

FIGURE 4: Secondary structure modification map of the HTLV-I DIS. Chemical and enzymatic modification data were combined with computer models to produce a structural map of the HTLV-I DIS. Open circles, lead acetate cleavage; black triangles, strong DMS modification; gray triangles, weaker DMS modification; solid circles, RNAse T1 cleavage; solid boxes, strong RNAse V1 cleavage; gray boxes, weak RNAse V1 cleavage; bold open boxes, strong RNAse U2 cleavage; open boxes, weak RNAse U2 cleavage.

A737 (Figure 2, lane 10), but only at an active concentration of 4 mM. Further modification of the downstream residues at positions 743−748, 750, 753, 755, and 757 was also observed following an increased duration of chemical exposure (data not shown), suggesting that this region may be predominantly single-stranded. This supposition was further supported by the extensive modification of the adenines downstream of A746 by DMS (Figure 2, lanes 11 and 12). Within the DIS, DMS produced clear modification of A737. These observations were reiterated by the use of DEPC (data not shown). An apparent modification of A740 at 10% DMS did not occur at 30% DMS and was not reproducible.

To further investigate the structural conformation of the HTLV-I DIS, end-labeled RNA714-828 was enzymatically modified with both RNAse V1 and RNAse U2. RNAse V1 produced extensive modification of the proposed helical stem from nucleotides C731−C735 and G739−G743, with particularly strong RT termination (template cleavage) mapping to positions U734, G739, and A740 (Figure 3, lanes 2 and 3). Additionally, cleavage was observed at positions C736 and G738, but not at A737, further supporting the data from the primer extensions. RNAse V1 cleavage also extended past the predicted 3′ termini of the DIS helical stem up to position U747. RNAse U2 modification induced strong cleavage at A737 (Figure 3, lane 5). In addition, much weaker cleavage of nucleotides G739−A746 was observed, implying possible structural flexibility within the region.

Molecular Modeling of the DIS. RNA secondary structures were mathematically modeled using mfold (*27*, *28*). Three-dimensional tertiary structure models were generated and fully energy-minimized using the molecular modeling software JUMNA (*29*), including an implicit solvation model (*30*) (Figure 5). The hairpin stem structure was modeled as an A-form helix. A noncanonical U:synG base pair, as found in the UUCG tetraloop (*31*), served as a basis for building a nearly isosteric C_{736}:synG_{738} base pair to close the trinucleotide loop.

Phylogenetic Conservation of the HTLV-I DIS. The above structural probing experiments were performed on the Caribbean viral isolate HTLV-I_{CH} (*32*). Although HTLV-I

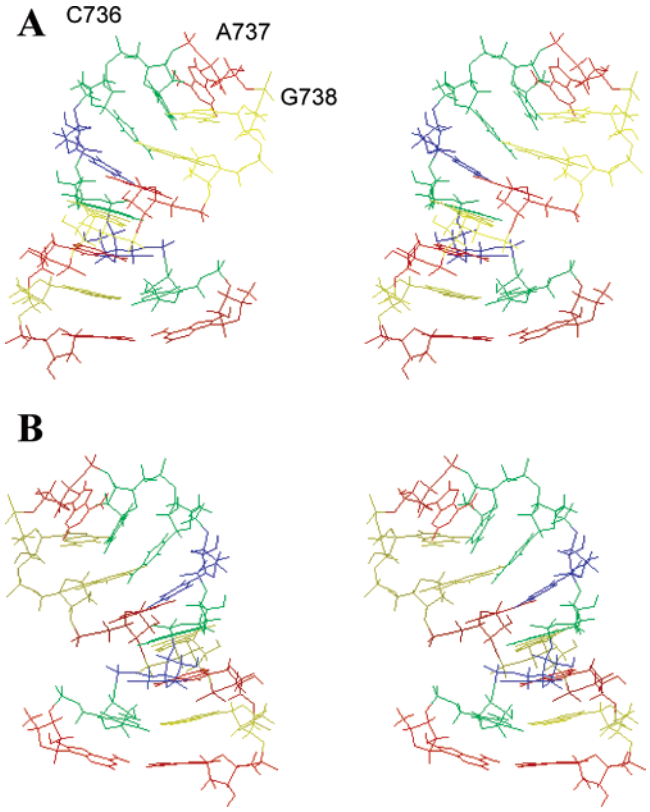

FIGURE 5: Potential three-dimensional structure of the HTLV-I DIS. Stereoview of 3D molecular modeling of a potential tertiary structure of the HTLV-I DIS using JUMNA (*29*). Bases are colored as follows: adenine, red; cytosine, green; guanine, yellow; and uracil, blue. Within the model, the O_2 atom of C_{736} is located at a similar position relative to G_{738} as the U:O_2 in the template U:synG base pair (*31*). The resulting hydrogen-bonding pattern is identical to that in the template. In the final energy-minimized model, the A_{737} base stacks on the C_{736}. Panel B is rotated 180° through the *y*-axis relative to panel A.

sequence heterogeneity within isolates is limited, distinct mutations identifying individual strains can be identified. If the HTLV-I DIS sequence is critical for dimerization, one would expect a high degree of conservation across HTLV-I isolates. Of 101 HTLV-I sequences identified from the EMBL database that contained leader sequences which included the DIS domain, 90 showed sequence identity with HTLV-I_{CH}. The other 11 sequences comprised three different mutational variants. Eight isolates contained a deletion of C736, two possessed the substitution A737G, and one possessed the substitution C733U. The substitution mutants are predicted to have a minimal impact on regional secondary structure, while the C736 deletion may induce formation of a terminal CAGG tetraloop (data not shown). Interestingly, a BlastN (v2.2) search using the mutant sequences revealed that A737G DIS possesses homology with almost 150 deposited HTLV-II leader sequences, suggesting a structural conservation for the DIS between HTLV-I and HTLV-II.

DISCUSSION

The minimal RNA sequence required for HTLV-I in vitro RNA dimerization is encompassed within nucleotides 730−743 (*19*). Biochemical probing of monomeric viral RNA indicates that the structural motif forming the DIS is atypical of previously identified DIS structures and does not present a loop sequence conducive to kissing-hairpin interactions.

The pattern of biochemical modification suggests that the DIS itself (nucleotides 731−743) forms a stem−loop structure closed by a single unpaired adenine residue. The poor reactivity of the DIS to single-stranded modifying agents, except for position A737 (Figure 2), its extensive cleavage by RNAse V1 (Figure 3), and the modification of A730 and A744 by single-strand-specific chemicals all imply the formation of a stem−loop with a closing C731:G743 base pair. The high sensitivity of A737 to DMS, U2 hydrolysis, and particularly lead acetate (Figures 2 and 3) indicates that this residue is unpaired and highly exposed in solution, consistent with a position as a terminal loop nucleotide. Further, the enhanced reactivity of A737 to lead acetate cleavage relative to other nucleotides may indicate possible involvement in magnesium binding. Certainly, magnesium stabilizes formation of the HTLV-I dimer (Greatorex, unpublished observations), and adenine bulges within the HIV-1 extended duplex have been identified as magnesium binding sites by crystallography (*33*). A role for A737 in magnesium binding could lead to formation of an analogous adenosine bulge in the HTLV-I RNA dimer.

The region downstream of the DIS is susceptible to a variety of single-strand-specific probes (Figure 2), and the arrangement of modification makes the presence of a specific structural motif unlikely. However, there may be further regions of base-pairing in close proximity to the DIS, as RNAse V1 showed modification up to position U747 (Figure 4). While this may be indicative of a potentially extended helical stem to the DIS, it could also either reflect structural flexibility in the context of RNA714-828, or be the result of this enzyme's ability to cleave nucleotides adjacent to helical domains (*34*).

The predicted structure for the DIS motif shown in Figure 4 postulates the formation of a C736:G738 base pair, rather than the formation of a closing trinucleotide loop. This proposition is based on the differing patterns of modification for the three residues forming the loop terminus, C736, A737, and G738. Unlike A737, neither C736 nor G738 shows susceptibility to single-strand-specific modification (Figure 2), but both were weakly cleaved by RNAse V1 (Figure 3). While this is suggestive of a base-pairing interaction, it is also plausible that this observation may result from steric hindrance due to stacking interactions at the top of the helix, or a reversion of the RNA to dimer. However, studies of the HIV-1 leader region have suggested that at least 95% of monomeric RNA remains so during modification (*35*); hence, any structural data originating from dimeric RNA should make a negligible contribution. Any base-pairing interaction between C736 and G738 would have to overcome the potential steric strain required for a single nucleotide to close the helix. Consequently, a standard Watson−Crick base pair is unlikely, as the distance between sugar C_1' atoms would be ~11 Å, and hence closure of such a gap by a single adenine residue would necessitate high levels of structural strain. However, if G738 adopts a syn conformation comparable with that in the UUCG tetraloop (*31*), the corresponding $C_1'-C_1'$ distance would be reduced to ~8.6 Å, such that a single adenine could close the helix without steric conflict. Molecular modeling demonstrates that these bonding interactions are sterically feasible (Figure 5). Such a conformation would also display partial structural homology to the AUA trinucleotide loop of brome mosaic virus (*21*), in which the first nucleotide of the loop is pushed out into solution, while the latter two are partially stacked upon the closing base pair below the loop. Further structural studies are ongoing to address the precise conformation of the DIS loop and also the bonding interactions present in dimeric RNA.

The HTLV DIS differs in sequence and structure from that of previously proposed core DIS motifs. Dimer linkages for HIV-1 (*15*, *16*), HIV-2 (*36*), and MoMuLV (*13*, *37*) all imply a critical role for short autocomplementary sequences exposed in the terminal loop of an RNA stem. HTLV-I does not possess such a loop, and except for A737, the entire HTLV DIS is autocomplementary. While one cannot rule out such interactions involving HTLV-I C736 and G738, they are unlikely and are not supported by the stability of HTLV-1 RNA dimers in the presence of EDTA and the absence of specific thermal treatment. Certainly, the dissociation of kissing hairpin dimers in the presence of EDTA, as recently demonstrated for HIV-2 (*38*), is not seen with HTLV-I. The triloop is present in over 90% of HTLV-1 sequences, but for dimer formation complementarity between strands is the critical requirement. We propose that a novel C−G pairing is one way in which retroviruses achieve stability in a critical hairpin. In the less common tetraloop, the same might be accomplished using the additional C−G canonical pair to close the loop with a two-base loop remaining.

The secondary structure of the HTLV-I DIS may indicate a novel mechanism for RNA dimer formation and may be a single-step process, possibly with immediate extended duplex formation. The high degree of sequence conservation and similarity to the DIS region across other primate deltaviruses suggests that this mechanism is conserved across the group.

ACKNOWLEDGMENT

We thank Teresa Wallman for secretarial assistance.

REFERENCES

1. Paillart, J. C., Marquet, R., Skripkin, E., Ehresmann, C., and Ehresmann, B. (1996) Dimerization of retroviral genomic RNAs−structural and functional implications, *Biochimie 78*, 639−653.
2. Greatorex, J., and Lever, A. (1998) Retroviral RNA dimer linkage, *J. Gen. Virol. 79*, 2877−2882.
3. Berkhout, B., and van Wamel, J. L. B. (1996) Role of the DIS hairpin in replication of Human Immunodeficiency Virus Type 1, *J. Virol. 70*, 6723−6732.
4. McBride, M. S., and Panganiban, A. T. (1996) The human immunodeficiency virus type 1 encapsidation site is a multipartite RNA element composed of functional hairpin structures, *J. Virol. 70*, 2963−2973.
5. Paillart, J. C., Berthoux, L., Ottmann, M., Darlix, J. L., Marquet, R., Ehresmann, B., and Ehresmann, C. (1996) A dual role of the putative RNA dimerization initiation site of human immunodeficiency virus type 1 in genomic RNA packaging and proviral DNA synthesis, *J. Virol. 70*, 8348−8354.
6. Ly, H., Nierlich, D. P., Olsen, J. C., and Kaplan, A. H. (2000) Functional characterization of the dimer linkage structure RNA of Moloney murine sarcoma virus, *J. Virol. 74*, 9937−9945.
7. Mikkelsen, J. G., Lund, A. H., Duch, M., and Pedersen, F. S. (2000) Mutations of the kissing-loop dimerization sequence influence the site specificity of murine leukemia virus recombination in vivo, *J. Virol. 74*, 600−610.
8. Bieth, E., Gabus, C., and Darlix, J.-L. (1990) A study of the dimer formation of Rous sarcoma virus RNA and of its effect on viral protein synthesis *in vitro*, *Nucleic Acids Res. 18*, 119−127.
9. Clever, J. L., and Parslow, T. G. (1997) Mutant human immunodeficiency virus type 1 genomes with defects in RNA dimerization or encapsidation, *J. Virol. 71*, 3407−3414.

10. Liang, C., Rong, L., Laughrea, M., Kleiman, L., and Wainberg, M. A. (1998) Compensatory point mutations in the human immunodeficiency virus type 1 gag region that are distal from deletion mutations in the dimerization initiation site can restore viral replication, *J. Virol. 72*, 6629−6636.
11. Liang, C., Rong, L., Quan, Y., Laughrea, M., Kleiman, L., and Wainberg, M. A. (1999) Mutations within four distinct gag proteins are required to restore replication of human immunodeficiency virus type 1 after deletion mutagenesis within the dimerization initiation site, *J. Virol. 73*, 7014−7020.
12. Ly, H., Nierlich, D. P., Olsen, J. C., and Kaplan, A. H. (1999) Moloney murine sarcoma virus genomic RNAs dimerize via a two-step process: a concentration-dependent kissing-loop interaction is driven by initial contact between consecutive guanines, *J. Virol. 73*, 7255−7261.
13. Girard, P.-M., Bonnet-Mathoniere, B., Muriaux, D., and Paoletti, J. (1995) A short autocomplementary sequence in the 5′ leader region is responsible for dimerization of MoMuLV genomic RNA, *Biochemistry 34*, 9785−9794.
14. Laughrea, M., and Jette, L. (1996) Kissing-Loop Model Of HIV-1 Genome Dimerization−HIV-1 RNAs Can Assume Alternative Dimeric Forms, and All Sequences Upstream or Downstream Of Hairpin 248−271 Are Dispensable For Dimer Formation, *Biochemistry 35*, 1589−1598.
15. Paillart, J. C., Skripkin, E., Ehresmann, B., Ehresmann, C., and Marquet, R. (1996) A loop-loop "kissing" complex is the essential part of the dimer linkage of genomic HIV-1 RNA, *Proc. Natl. Acad. Sci. U.S.A. 93*, 5572−5577.
16. Skripkin, E., Paillart, J. C., Marquet, R., Ehresmann, B., and Ehresmann, C. (1994) Identification of the primary site of the human immunodeficiency virus type 1 RNA dimerization in vitro, *Proc. Natl. Acad. Sci. U.S.A. 91*, 4945−4949.
17. Greatorex, J. S., Laisse, V., Dokhelar, M.-C., and Lever, A. M. L. (1996) Sequences involved in the dimerisation of human T-cell leukaemia virus type-1 RNA, *Nucleic Acids Res. 24*, 2919−2923.
18. Le Blanc, I., Greatorex, J., Dokhelar, M.-C., and Lever, A. M. L. (2000) A 37 base sequence in the leader region of human T-cell leukaemia virus type 1 is a high affinity dimerization site but is not essential for virus replication, *J. Gen. Virol. 81*, 105−108.
19. Monie, T., Greatorex, J., and Lever, A. M. L. (2001) Oligonucleotide mapping of the core dimer linkage in HTLV-1, *Virus Res. 78*, 45−56.
20. Klinck, R., Westhof, E., Walker, S., Afshar, M., Collier, A., and Aboul-Ela, F. (2000) A potential RNA drug target in the hepatitis C virus internal ribosomal entry site, *RNA 6*, 1423−1431.
21. Kim, C. H., Kao, C. C., and Tinoco, I., Jr. (2000) RNA motifs that determine specificity between a viral replicase and its promoter, *Nat. Struct. Biol. 7*, 415−423.
22. Battiste, J. L., Mao, H., Rao, N. S., Tan, R., Muhandiram, D. R., Kay, L. E., Frankel, A. D., and Williamson, J. R. (1996) Alpha helix-RNA major groove recognition in an HIV-1 rev peptide-RRE RNA complex, *Science 273*, 1547−1551.
23. Joost Haasnoot, P. C., Olsthoorn, R. C., and Bol, J. F. (2002) The Brome mosaic virus subgenomic promoter hairpin is structurally similar to the iron-responsive element and functionally equivalent to the minus-strand core promoter stem-loop C, *RNA 8*, 110−122.
24. Mujeeb, A., Clever, J. L., Billeci, T. M., James, T. L., and Parslow, T. G. (1998) Structure of the dimer initiation complex of HIV-1 genomic RNA, *Nat. Struct. Biol. 5*, 432−436.
25. Ennifar, E., Walter, P., Ehresmann, B., Ehresmann, C., and Dumas, P. (2001) Crystal structures of coaxially stacked kissing complexes of the HIV-1 RNA dimerization initiation site, *Nat. Struct. Biol. 8*, 1064−1068.
26. Harrison, G. P., Mayo, M. S., Hunter, E., and Lever, A. M. L. (1998) Pausing of reverse transcriptase on retroviral RNA templates is influenced by secondary structures both 5′ and 3′ of the catalytic site, *Nucleic Acids Res. 26*, 3433−3442.
27. Mathews, D. H., Sabina, J., Zuker, M., and Turner, D. H. (1999) Expanded sequence dependence of thermodynamic parameters improves prediction of RNA secondary structure, *J. Mol. Biol. 288*, 911−940.
28. Zuker, M., Mathews, D. H., and Turner, D. H. (1999) in *RNA Biochemistry and Biotechnology* (Barciszewski, J., and Clark, B. F. C., Eds.) pp 11−43, NATO ASI Series, Kluwer Academic Publishers.
29. Lavery, R., Zakrzewska, K., and Sklenar, H. (1995) JUMNA (Junction Minimisation of Nucleic Acids), *Comput. Phys. Commun. 91*, 135−158.
30. Zacharias, M. (2001) Conformational analysis of DNA-trinucleotide-hairpin-loop structures using a continuum solvent model, *Biophys. J. 80*, 2350−2363.
31. Varani, G., Cheong, C., and Tinoco, I., Jr. (1991) Structure of an unusually stable RNA hairpin, *Biochemistry 30*, 3280−3289.
32. Ratner, L., Philpott, T., and Trowbridge, D. B. (1991) Nucleotide sequence analysis of isolates of human T-lymphotropic virus type 1 of diverse geographical origins, *AIDS Res. Hum. Retroviruses 7*, 923−941.
33. Ennifar, E., Yusupov, M., Walter, P., Marquet, R., Ehresmann, B., Ehresmann, C., and Dumas, P. (1999) The crystal structure of the dimerization initiation site of genomic HIV-1 RNA reveals an extended duplex with two adenine bulges, *Struct. Fold. Des. 7*, 1439−1449.
34. Kean, J. M., and Draper, D. E. (1985) Secondary structure of a 345-base RNA fragment covering the S8/S15 protein binding domain of *Escherichia coli* 16S ribosomal RNA, *Biochemistry 24*, 5052−5061.
35. Damgaard, C. K., Dyhr Mikkelsen, H., and Kjems, J. (1998) Mapping the RNA binding sites for human immunodeficiency virus type 1 Gag and NC proteins within the complete HIV-1 and -2 untranslated leader regions, *Nucleic Acids Res. 26*, 3667−3676.
36. Dirac, A. M., Huthoff, H., Kjems, J., and Berkhout, B. (2001) The dimer initiation site hairpin mediates dimerization of the human immunodeficiency virus, type 2 RNA genome, *J. Biol. Chem. 276*, 32345−32352.
37. Ly, H., and Parslow, T. G. (2002) Bipartite signal for genomic RNA dimerization in Moloney murine leukemia virus, *J. Virol. 76*, 3135−3144.
38. Lanchy, J. M., and Lodmell, J. S. (2002) Alternate usage of two dimerization initiation sites in HIV-2 viral RNA in vitro, *J. Mol. Biol. 319*, 637−648.

BI030237I